http://dx.doi.org/10.5012/bkcs.2012.33.12.4165

Fluorescent Magnetic Silica Nanotubes with High Photostability Prepared by the Conventional Reverse Micro-Emulsion Method

Yuhai Zhang and Sang Jun Son*

*Department of Chemistry, Gachon University, Seongnam, Gyeonggi 461-701, Korea. *E-mail: sjson@gachon.ac.kr*
Received November 3, 2012, Accepted November 6, 2012

Magnetic fluorescent silica nanotubes were fabricated using reverse micro-emulsions coupled with conventional sol-gel methods. Anodic aluminum oxide templates were used to separate spatially the magnetic and the fluorescent moieties on individual nanotubes and so prevent quenching of the fluorescence. C18 and fluorescent layers were deposited sequentially on silica. Magnetism was then obtained by the introduction of pre-made magnetic nanoparticles inside the nanotubes. The photo- and chemical stabilities of nanotubes were demonstrated through dye release and photobleaching tests. The produced nanotubes did not show fluorescence quenching upon the addition of the nanoparticles, an advantage over conventional spherical fluorescent magnetic nanoparticles. High photostability of nanotubes, magnetism and biocompatiblily make them potentially useful in bioanalysis.

Key Words : Silica nanotube, Magnetic, Fluorescent, Dual functionality, Fluorescence quenching

Introduction

The development of multifunctional nanomaterials would aid various clinical processes, such as bioimaging, drug delivery and cancer therapy.[1-3] Fluorescent nanoparticles can be used for imaging and to allow observation of biological events. The use of nanoparticles with magnetic properties can enable separation, signal-amplified detection and MR imaging. The combination of magnetic nanoparticles and fluorescent materials (dyes or QDs) in single nanoparticles has been attempted in structures such as embedded nanoparticles,[4] dumbbells[5] and core/shell particles.[6] However, simple syntheses such as the co-doping of magnetic nanoparticles and QDs in silica or other organic/bioorganic polymer matrices places both components close to each other, and leads the magnetic particles to cause optical interference or to decrease fluorescence.[7] The fabrication of bifunctional magnetic and fluorescent nanoparticles remains a challenge.

Spherical silica nanoparticles are promising bases for nanocomposites because of their biocompatibility and optical properties[4-7]; tubular structures have been studied much less. However, silica nanotubes have some obvious advantages over spherical nanoparticles: they have inner and outer surfaces which can be differentially modified and their inner voids can act as containers for molecules.[8,9] Therefore, they are attractive alternatives to spherical nanoparticles for overcoming the problems facing the development of multifunctional nanomaterials.

This work describes a novel fabrication method of magnetic fluorescent silica nanotubes using reverse micro-emulsions and layer-by-layer processing. It allowed the placement control of each functional substance to avoid interference between the magnetic and the fluorescent moieties (Scheme 1). First, fluorescent nanotubes were prepared by the sequential deposition of three layers onto lab-made anodic aluminum oxide templates: silica, C18 and a fluorophore. Each layer's role was investigated through the fabrication of silica nanotubes with different combinations of the three layers. Magnetic properties were introduced using pre-made magnetic nanoparticles which were placed inside the nanotubes by refluxing. After removal of the template to give free standing bifunctional nanotubes, dye release and photostability were assessed.

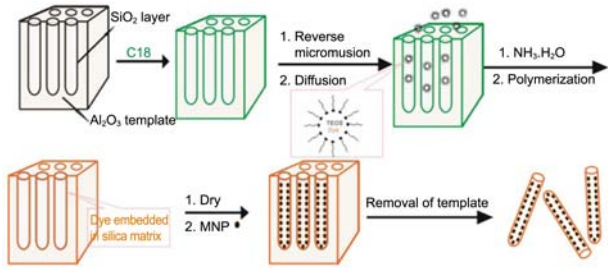

Scheme 1. The synthesis of magnetic and fluorescent silica nanotubes. Black, silica; green, C18; and yellow, fluorescent dye.

Experimental

Materials. Silicon tetrachloride ($SiCl_4$, 99.8%, Acros Organics), perchloric acid (70%, DC Chemical), *n*-octadecyltrimethoxysilane (C18-silane, 95%, Sigma), *N,N*-diisopropylethyl amine (DIEA, Aldrich, 99.5%), tetraethoxysilane (TEOS, Aldrich, 98%), ammonium hydropxide (Daejung, 25%) and aluminum oxide (fused, −325 mesh, +10 micron, 99%, Aldrich) were used as received. Aluminum foil (99.99%) was purchased from Alfa Aesar (Ward Hill, MA, USA).

Deposition of Silica Layer: An anodic aluminum oxide template with 5 mm pore depth was prepared by established methods.[10] A silica layer was deposited through a surface sol-gel method.[11,12] Briefly, one cycle of sol-gel processing

involved immersing the templates in $SiCl_4$ (99.8%) solution for 5 min, washing them with hexane and methanol, drying them, immersing them in DI water for 5 min and washing them with methanol. Five such cycles produced a silica layer of optimal thickness (*ca.* 8 nm).

Deposition of C18: Templates both with and without sol-gel processing were separately placed in 25-mL round-bottomed flasks. Toluene (10 mL), trimethoxy(octadecyl)-silane (C18-silane, 3 mL) and *N,N*-diisopropylethylamine (0.1 mL) were added to the templates and heated under reflux for 2 h. After cooling to room temperature, the templates were washed twice with methanol and dried in air.

Deposition of Fluorescent Layer: A microemusion was prepared by a slight modification of a reported method.[13] In brief, TritonX-100 (1.77 mL) and cyclohexane (7.5 mL) were vigorously stirred in a 20 mL glass vial. Fluorescent dye, Rhodamine B (3.0 mg), in 95% aqueous ethanol (1.0 mL) was added dropwise followed by the addition of 80 μL TEOS. After 20 min, the templates with Rhodamine B in their pores were soaked in the microemusion under vigorous stirring. After 30 min, NH_4OH (60 μL) was added to initiate polymerization. The reaction was allowed to continue for 24 h at room temperature in darkness. The resulting templates were washed with water and dried in air.

Preparation of the Au-capped F-SNT: Au-capped fluorescent nanotubes were prepared as a control by an established method.[14] The template with embedded nanotubes was soaked in methanol containing Rhodamine B (0.03%, wt/v), and dried before a 70 nm gold layer was deposited by thermal evaporation at 0.16 nm/s. Gold capping of the nanotubes was achieved by shaking the template and commercial alumina powder for 2 days. Free-standing Au-capped nanotubes were obtained by dissolving the template in 0.1 M NaOH for 20 min, followed by filtering in a centrifugal filter (Millipore, 0.5 μm) and collected in D.I. water.

Preparation of Fe_3O_4 Nanoparticles: Fe_3O_4 nanoparticles were prepared hydrothermally. In typical procedure, sodium oleate (2.4 g), oleic acid (3 mL), ethanol (15 mL) and D.I. water (10 mL) were mixed at 50 °C to form a yellow colloid. 0.54 g $FeCl_3$ and 0.20 g $FeCl_2$ in 10 mL aqueous solution were added under vigorous stirring. The mixture was sealed in a Teflon tube and heated to 160 °C. The reaction was allowed to proceed for 4 h before being cooled to room temperature. A dark unsuspended precipitate product was collected using cyclohexane and precipitated using excess ethanol. The washing was repeated twice before drying in vacuum.

Modification with Preformed Magnetic Nanoparticles: The hydrothermally synthesized magnetic Fe_3O_4 nanoparticles were purified and dispersed in toluene (5 mg/mL).[15] Template containing fluorescent nanotubes was soaked in the Fe_3O_4 suspension and heated under reflux for 2 h under argon. The template was then washed with toluene and dried in air.

Removal of Template to Obtain Freestanding Nanotubes: The nanotubes and templates were mechanically polished in aluminia powder and dissolved in 0.1 M NaOH for 20 min. The resulting freestanding nanotubes were filtered in a centrifugal filter (Millipore, 0.5 μm) and collected in D.I. water.

Release Test: Aluminum oxide templates (0.60 cm^2) were soaked in 2.0 mL water in a plastic tube. 80 mL aliquots were intermittently taken for sampling. After 4 days' incubation, the templates were dissolved in NaOH, leaving freestanding nanotubes which were collected in water and measured, like the other collected samples, under a fluorescence microplate reader (Perkin-Elmer VICTOR3 1420 Multilabel Counter) with a 543 nm excitation filter and a 572 nm emission filter. Summing all the recorded fluorescence intensities, including from the freestanding nanotubes, allowed determination of the total amount of dye. Concentrations were calculated based on a standard curve of Rhodamine B.

Photobleaching Test: Fluorescent nanotubes, both Au capped and sidewall doped, were separately dried on glass slides. They were focused under a confocal microscope under continuous laser excitation (543 nm, gain 50%). Spectra were recorded through attached software every minute for 20 min. The peak of each spectrum was recorded and normalized as the emission intensity.

Measurements: Samples' morphologies were examined by field emission scanning electron microscopy (FE-SEM, JEOL JSM-6700F) and transmission electron microscopy (TEM, HITACHI H-7100). Optical microscopy images (bright field, dark field and fluorescence) were recorded using a confocal microscope (Nikon, D-eclipse C1si) and fluorescent microscope (Nikon, eclipse 80i). Fluorescence intensities were compared using consistent microscope settings: filter (Ex510-560, DM575, and BA590), exposure time (100 ms) and gain value (1.0). TEM and SEM samples were prepared by drying sample solutions on copper grids and carbon tape, respectively.

Results and Discussion

Figure 1 shows TEM, bright field optical microscopy and fluorescence microscopy images of the four sets of nanotubes composed of different layers. Silica layers were prepared on lab-made nanoporous anodic aluminum oxide templates by surface sol-gel processing.[16] The inner surfaces of nanotubes were then selectively modified with octadecyl triethoxy silane (C18-silane) to prepare a hydrophobic environment. Fluorescent layers were prepared using a modified reverse microemulsion method.[17] A reverse microemulsion is a thermal dynamic stable system which consists of small water-in-oil droplets. Here, the droplets contained a polar liquid core (EtOH, H_2O, TEOS and Rhodamine B), a non-polar liquid shell (cyclohexane) and a mediating surfactant layer (Triton X-100). After the droplets had diffused into the pores of the template, ammonia was added to trigger the polymerization of TEOS, which trapped the dye in the silica matrix. The thickness of the fluorescent layer was measured by TEM to be *ca.* 1-2 nm.

Although the nanotubes with sol-gel processed layers (TEM images Figures 1(a) and 1(c)) exhibited well-defined

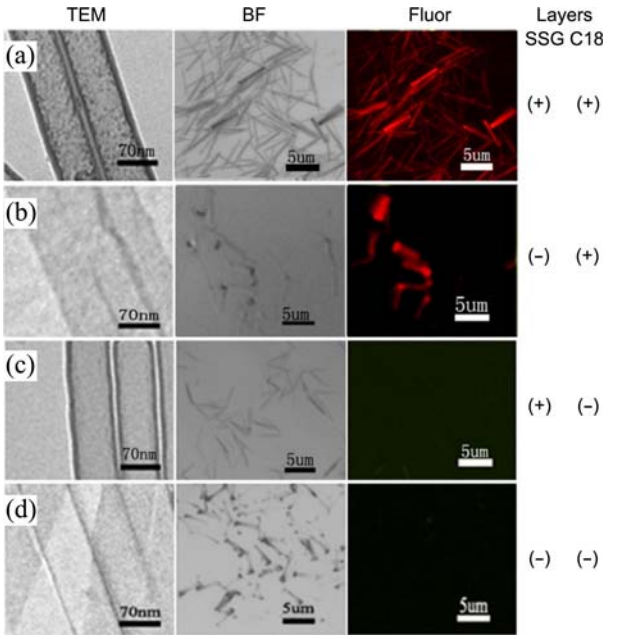

Figure 1. TEM and optical microscopy images in bright field (BF) and fluorescent mode (Fluor) of silica nanotubes prepared using different combinations of layers: (a) Silica, C18 and fluorescent layers. (b) C18 and fluorescent layers. (c) Silica and fluorescent layers. (d) Only fluorescent layer. + indicates with sol-gel processing or C18 treatment; – represent without treatment.

wall thicknesses, fluorescence was detected only from the samples with a C18 layer. This implies that the hydrophobic C18 layer was necessary for the trapping and retention of the fluorescent dye. The C18 layer facilitated interactions with the micro-emulsion droplets allowing their diffusion into the pores by offering a hydrophobic environment compatible with their dispersing medium. The C18 layer could also protect the trapped dyes from being released into the aqueous media used in the experiment.

The enhanced photostability of the fluorescent dye by the silica matrix was tested through photobleaching by exposing the nanotubes to a laser continuously for 1200 s. As a control, Au-caped nanotubes containing Rhodamine B inside the tubes' voids were prepared by a reported method.[14] Less than 20% of the fluorescent intensity was lost when dye was entrapped in the side-walls of the nanotubes, whereas dye encapsulated in the nanotubes' voids significantly decreased (Figure 2(a)). This indicates that the silica matrix showed a shielding effect similar to that reported by Tan *et al.*[17] for silica nanoparticles, which separated and isolated dye molecules from surrounding local environments, such as H_2O or O_2. Dye was determined to be contained in the inner void of the Au-capped control nanotubes rather than being captured in their silica matrix. Therefore, shielding by the matrix was not expected to be as strong as when dye was located in the nanotubes' side walls.

Dye release from the nanotubes with and without C18 was tested while the tubes were still embedded in the template. The proportion of dye released from the tubes was measured after different durations of exposure to water (Figure 2(b)).

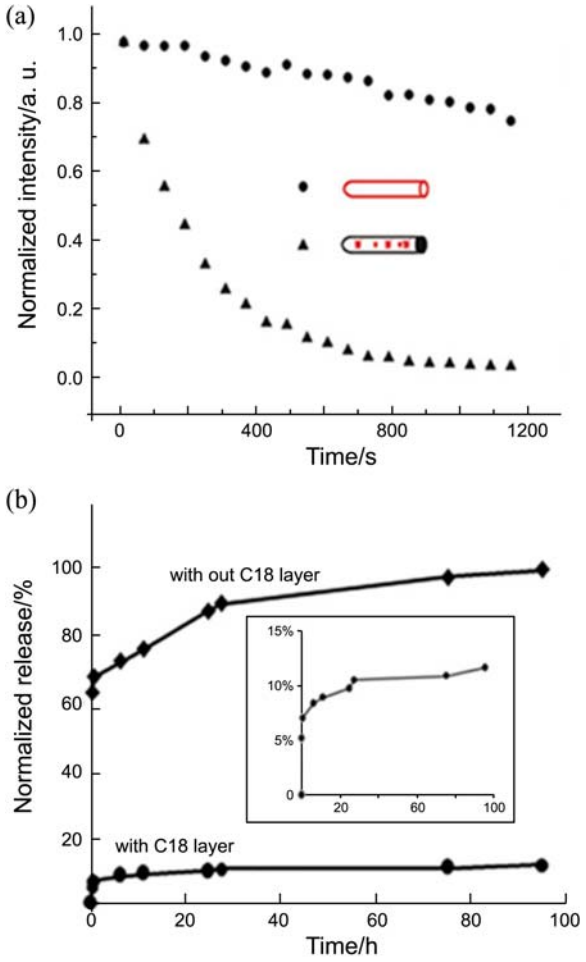

Figure 2. (a) Photobleaching of fluorescent nanotubes with dye either entrapped in the tubes' side walls or voids. (b) Dye release tests of fluorescent nanotubes with and without C18 layers.

Assuming that the Rhodamine B was only either released or retained, only *ca.* 18% was released from the nanotubes containing C18 after 4 days' incubation in water and no further release was observed after reaching saturation. The nanotubes without C18 lost most of the dye within hours, demonstrating that C18 was required not only for the deposition of the fluorescent layer, but also for its retention. The fact that the loss of dye from the nanotubes with C18 did not increase significantly after several hours implies that relatively long-term storage of the nanotubes in aqueous solutions is possible. The dye release experiments allowed estimation of the amount of Rhodamine B inside the nanotubes by summing the fluorescence intensities of the dye released from the tubes. 1.9 nmol Rhodamine B was trapped in 8.7×10^9 nanotubes, *i.e.* 1.3×10^6 molecules in per nanotube, a value in agreement with the reported loading of silica nanoparticles.[17]

To prepare magnetic fluorescent nanotubes, pre-made magnetic Fe_3O_4 nanoparticles with hydrophobic oleic acid coatings were introduced under reflux to the fluorescent nanotubes with the template. The initially smooth inner walls of the fluorescent nanotubes (Figure 3(a)) became densely packed with nanoparticles in the free standing bifunctionized

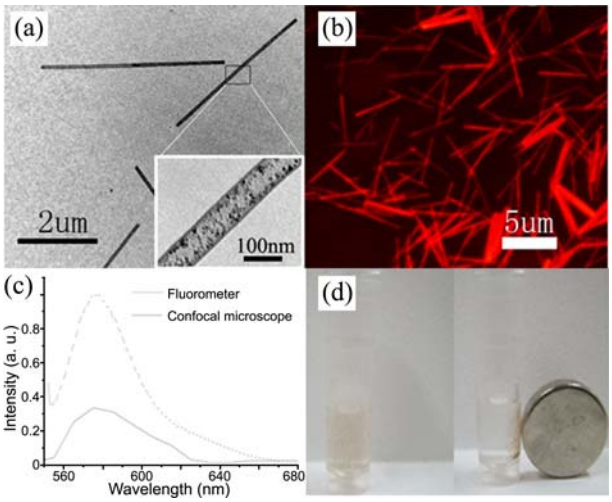

Figure 3. (a) TEM image (inset, a magnified image) and (b) fluorescent microscopy image of bifunctional magnetic and fluorescent nanotubes; (c) the tubes' emission spectra measured in bulk solution using a fluorometer (solid line) and confocal microscope (dashed line); (d) the tubes' magnetic separation under a magnetic field.

nanotubes obtained after dissolving the template. The nanoparticles were well distributed inside the nanotubes and did not appear to stack close to the tubes' ends. The addition of hydrophobic nanoparticles to nanotubes with hydrophobic C18-silane interiors led to the stacking of the particles inside the tubes. The distribution of particles inside the tubes shows that the first deposited hydrophobic C18 layer was overlaid by a hydrophilic fluorescent layer, which arose because the inner fluorescent layer was prepared using a reversed microemulsion with hydrophilic outer surfaces.

The fluorescence of dyes located close to inorganic nanoparticles tends to be quenched by the particles.[7] The bifunctional tubes contained fluorescence dye and nanoparticles close to each other but showed no significant loss of fluoresce upon addition of the particles (Figure 3(b)). The silica matrix of the nanotubes' side walls likely separated the nanoparticles from the entrapped dye and prevented both excitation and emission radiation from being absorbed by the nanoparticles. This is the major advantage of bifunctional nanotubes over spherical magnetic and fluorescent nanoparticles. The fluorescence spectrum of Rhodamine B was retained after the dye was entrapped in the nanotubes' side walls (Figure 3(c)).

Magnetic separation of the bifunctionalized tubes was demonstrated (Figure 3(d)). The superparamagnetic Fe_3O_4,[18] which made the dispersion appear brown under no external magnetic field (left image), caused the particles to move towards a nearby magnet and so led the dispersion to lose its color. This indicates that the nanoparticles' magnetic properties were maintained inside the nanotubes and allowed the bifunctionalized tubes to display magnetic behavior.

Conclusion

Magnetic and fluorescent silica nanotubes were fabricated by layer-by-layer assembly. In the frame of the initial silica layer, C18 and a fluorophore were sequentially deposited. The C18 was required to allow the formation and retention of the fluorescent Rhodamine B dye. Dye entrapped in the silica matrix showed higher photostability than dye encapsulated in the nanotubes' voids. Magnetic nanoparticles were then introduced into the fluoresent nanotubes. They were well dispersed throughout the tubes, indicating that the initial hydrophobic surfaces of the nanotubes had become hydrophilic upon deposition of the fluorescent layer. The bifunctionalized nanotubes showed fluorescence that was not quenched by the magnetic nanoparticles, which represents a significant advantage over conventional spherical fluorescent magnetic nanoparticles. Given the advantages of high photostability, maganetism and biocompatiblily, these bifunctionalized nanotubes show potential applicability as probes for bioanalysis.

Acknowledgments. This study was supported by a grant from the Korea Research Foundation funded by the Korean Government (KRF-2011-0002138 and 2010-0022936).

References

1. Beck-Broichsitter, M.; Gauss, J.; Packhaeuser, C. B.; Lahnstein, K.; Schmehl, T.; Seeger, W.; Kissel, T.; Gessler, T. *Int. J. Pharm.* **2009**, *367*, 169.
2. Chang, I. P.; Hwang, K. C.; Chiang, C. S. *J. Am. Chem. Soc.* **2008**, *130*, 15476.
3. Huang, Y. F.; Chang, H. T.; Tan, W. *Anal. Chem.* **2008**, *80*, 567.
4. Wang, G. P.; Song, E. Q.; Xie, H. Y.; Zhang, Z. L.; Tian, Z. Q.; Zuo, C.; Pang, D. W.; Wu, D. C.; Shi, Y. B. *Chem. Commun.* **2005**, 4276.
5. Xie, H. Y.; Zuo, C.; Liu, Y.; Zhang, Z. L.; Pang, D. W.; Li, X. L.; Gong, J. P.; Dickinson, C.; Zhou, W. *Small* **2005**, *1*, 506.
6. Kim, H.; Achermann, M.; Balet, L. P.; Hollingsworth, J. A.; Klimov, V. I. *J. Am. Chem. Soc.* **2005**, *127*, 544.
7. Wang, G.; Wang, C.; Dou, W.; Ma, Q.; Yuan, P.; Su, X. *J. Fluoresc.* **2009**, *19*, 939.
8. Chen, C. C.; Liu, Y. C.; Wu, C. H.; Yeh, C. C.; Su, M. T.; Wu, Y. C. *Adv. Mater.* **2005**, *17*, 404.
9. (a) Zhang, L. L.; Lin, Y. M.; Zhou, H. C.; Wei, S. D.; Chen, J. H. *Molecules 15*, 420. (b) Yang, X.; Tang, H.; Cao, K.; Song, H.; Sheng, W.; Wu, Q. *J. Material Chem.* **2011**, *21*, 6122.
10. Masuda, H.; Fukuda, K. *Science* **1995**, *268*, 1466.
11. Kovtyukhova, N. I.; Mallouk, T. E.; Pan, L.; Dickey, E. C. *J. Am. Chem. Soc.* **2003**, *125*, 9761.
12. Kovtyukhova, N. I.; Mallouk, T. E.; Mayer, T. S. *Adv. Mater.* **2003**, *15*, 780.
13. Zhao, X. J.; Bagwe, R. P.; Tan, W. H. *Adv. Mater.* **2004**, *16*, 173.
14. Yu, J.; Bai, X.; Suh, J.; Lee, S. B.; Son, S. J. *J. Am. Chem. Soc.* **2009**, *131*, 15574.
15. Wang, X.; Zhuang, J.; Peng, Q.; Li, Y. D. *Nature* **2005**, *437*, 121.
16. Son, S. J.; Reichel, J.; He, B.; Schuchman, M.; Lee, S. B. *J. Am. Chem. Soc.* **2005**, *127*, 7316.
17. Zhao, X.; Tapec-Dytioco, R.; Tan, W. *J. Am. Chem. Soc.* **2003**, *125*, 11474.
18. Bai, X.; Son, S. J.; Zhang, X.; Liu, W.; Jordan, E. K.; Frank, J. A.; Venkatesan, T.; Lee, S. B. *Nanomedicine* **2008**, *3*, 163.